

Original Research

## Preparation & Characterization of Polyvinyl Alcohol-Sodium Alginate-Starch Based Hydrogel by Gamma Radiation and Its Application for the Treatment of Dye Containing Water

Depok Chandra Shil <sup>1,2</sup>, Nazia Rahman <sup>1,\*</sup>, Shahnaz Sultana <sup>1</sup>, Md. Nabul Sardar <sup>1</sup>, Puja Majumder <sup>2</sup>, Fataha Nur Robel <sup>2</sup>

1. Nuclear and Radiation Chemistry Division, Institute of Nuclear Science and Technology, Atomic Energy Research Establishment, Bangladesh Atomic Energy Commission, Dhaka, Bangladesh; E-Mails: [depoknstu@gmail.com](mailto:depoknstu@gmail.com); [naziabaec@gmail.com](mailto:naziabaec@gmail.com); [shahnazju32@gmail.com](mailto:shahnazju32@gmail.com); [nabilchemist.ru@gmail.com](mailto:nabilchemist.ru@gmail.com)
2. Department of Applied Chemistry and Chemical Engineering, Noakhali Science and Technology University, Noakhali, Bangladesh; E-Mails: [pujamajumder225@gmail.com](mailto:pujamajumder225@gmail.com); [fnobel.acce@nstu.edu.bd](mailto:fnobel.acce@nstu.edu.bd)

\* **Correspondence:** Nazia Rahman; E-Mail: [naziabaec@gmail.com](mailto:naziabaec@gmail.com)

**Academic Editor:** Mohammad Boshir Ahmed

**Special Issue:** [Advanced Materials and Technologies for Pollutants Removal and Environmental Remediation](#)

*Adv Environ Eng Res*

2023, volume 4, issue 4

doi:10.21926/aeer.2304048

**Received:** September 04, 2023

**Accepted:** October 25, 2023

**Published:** November 02, 2023

### Abstract

Hydrogels are three-dimensional, hydrophilic networks of polymers with a high water absorption capacity. We investigated the removal of monovalent cationic dye, methylene blue, from aqueous solutions by a polyvinyl alcohol/Sodium alginate/Starch mix hydrogel to discover a solution to the environmental waste-water problem. By applying a gamma radiation dose from a Co-60 source without adding a hazardous cross-linker, a novel PVA/SA/Starch mix hydrogel was synthesized. The effects of factors like irradiation dose and composition ratio on the manufactured hydrogel (PAS hydrogel) characteristics, including gel



© 2023 by the author. This is an open access article distributed under the conditions of the [Creative Commons by Attribution License](#), which permits unrestricted use, distribution, and reproduction in any medium or format, provided the original work is correctly cited.

content and swelling behavior, were carefully examined. At various radiation dosages, the cross-linking density of the PAS (PVA/SA/Starch) hydrogel was investigated. The 30 kGy was selected as the optimal dose based on swelling ratio and gel fraction, and 0.25% starch was chosen as the optimal starch content. By using FTIR, the produced hydrogel was identified. The ability of the hydrogel to remove methylene blue was investigated while taking isotherm and kinetic factors into account. The homogeneously distributed active sites on the surface of this hydrogel have undergone monolayer adsorption, according to fitting using the Langmuir model. This hydrogel offers promising potential for treating waste-water containing methylene blue dye solution.

### **Keywords**

Hydrogel; methylene blue; gamma radiation; swelling ratio; dye adsorption

## **1. Introduction**

Textile printing is responsible for environmental issues. Dyes, chemicals, and other ingredients are frequently found in textile printing and dye water [1, 2]. Some dyes might need greater care to prevent harming people's health [3]. To avoid any environmental problems, dye-containing water must be entirely and effectively treated. Due to their biodegradability and environmentally beneficial properties, natural inestimable polysaccharide materials like starch, chitosan, etc., have recently attracted interest for use as adsorbents in water treatment [4-6].

Starch is a biodegradable polymer. For decades, several starch derivatives with amide, amino, carboxyl, and other groups have been developed and used to clean water [7-9]. Combining two or more polymers is essential to create new biomaterials with enhanced capabilities that a single polymer cannot provide. PVA, a water-soluble polymer, biodegradable and non-toxic, has been incorporated into several blends for use in biomedical and water treatment applications [10, 11]. Another recognized candidate for a biodegradable polymeric material is a PVA/starch mixture [12].

The carboxyl groups in sodium alginates can be protonated or ionized, which aids in connecting with different groups [13, 14]. Because sodium alginate has a high concentration of -COO- groups, it can be a natural biodegradable absorbent for treating industrial waste-water, particularly for dye pollutants. Their reuse can help to prevent secondary pollution or other environmental problems [15].

The methods utilized for waste-water purification require the creation of operations using cutting-edge materials that are affordable and incredibly effective in removing pollutants. Hydrogels have recently demonstrated the potential for adsorbing contaminants from contaminated water [16]. A unique class of super absorbents called hydrogels may absorb thousands of times more water than their dry weight. They comprise three-dimensional networks of cross-linked polymeric chains joined by covalent or physical connections. Due to their wide range of uses, they have attracted a lot of attention lately [17, 18]. Hydrogel has many applications, including removing heavy metals and dyes from waste-water, tissue engineering, self-healing materials, biosensors, hemostasis bandages, and artificial organ production. The qualities that set hydrogel apart from other intelligent materials include its hydrophilicity, biocompatibility, and high swelling ratio.

Numerous studies on the use of hydrogel in various fields are now being conducted [19-22]. One recent study reviewed the removal of methylene blue from waste-water using hydrogel nanocomposite [23]. Another study reported preparing and applying super-adsorbent hydrogels to remove methylene blue from an aqueous solution [24]. Another example of methylene blue removal studies is the Removal of Methylene Blue Dye Using a Biodegradable Superabsorbent Hydrogel Polymer Composite Incorporated with Activated Charcoal [25]. Another review focuses on design of composite hydrogels for the remediation of dye-contaminated water and waste-water [26].

In the current study, Co-60 irradiation was used to create a novel hydrogel from polyvinyl alcohol/Sodium alginate/Starch blend (PVA/SA/Starch blend hydrogels). To our knowledge, no previous study reported the preparation of polyvinyl alcohol/Sodium alginate/Starch blend hydrogel and its application in dye removal. Using gamma radiation to prepare hydrogel is an environmentally friendly process as it requires no toxic cross-linking agent. This study investigated the effects of factors like irradiation dose and composition ratio on the manufactured hydrogel (PAS hydrogel) characteristics, including gel content, swelling behavior, and cross-linking density. By using FTIR, the produced hydrogel was identified. It was looked into whether the hydrogel might be used to remediate waste water, including methylene blue dye. The kinetics and isotherm properties of elimination of the methylene blue dye were also investigated.

## **2. Experimental**

### **2.1 Materials**

Fluka Chemicals, Germany, supplied polyvinyl alcohol (PVA). Chinese company UNI-CHEM Chemical Reagent provided the sodium alginate. Sigma Aldrich, USA, delivered the starch and sodium hydroxide. BDH, England, supplied the hydrochloric acid. All experiments utilized distilled water.

### **2.2 Preparation of Hydrogel**

The radiation cross-linking method was introduced to create the proposed hydrogel. A 5% PVA (w/v) aqueous solution was made and autoclaved for an appropriate period. The required amount of starch was dissolved under steady stirring at 180 rpm for 45 minutes at 80°C. Water was continuously stirred while 1% sodium alginate was dissolved at 200 rpm. PVA and starch solutions were combined with sodium alginate solution after both solutions were cooled to room temperature. To examine the impact of starch on the gel's characteristics, the starch composition was changed from 0 to 1% while keeping the PVA and alginate contents constant at 5% and 1%, respectively. The liquids were loaded into polyethylene plastic bags, sealed, and put in glass tubes to prepare the hydrogel. The samples were then given gamma radiation doses of 20-40 kGy from a Co-60 source (dose rate: 6.8 kGy/h). The hydrogels were then sliced into minute pieces, dried in the air, and then heated at 45°C until they reached a constant weight. The preparation process is displayed in Figure 1.

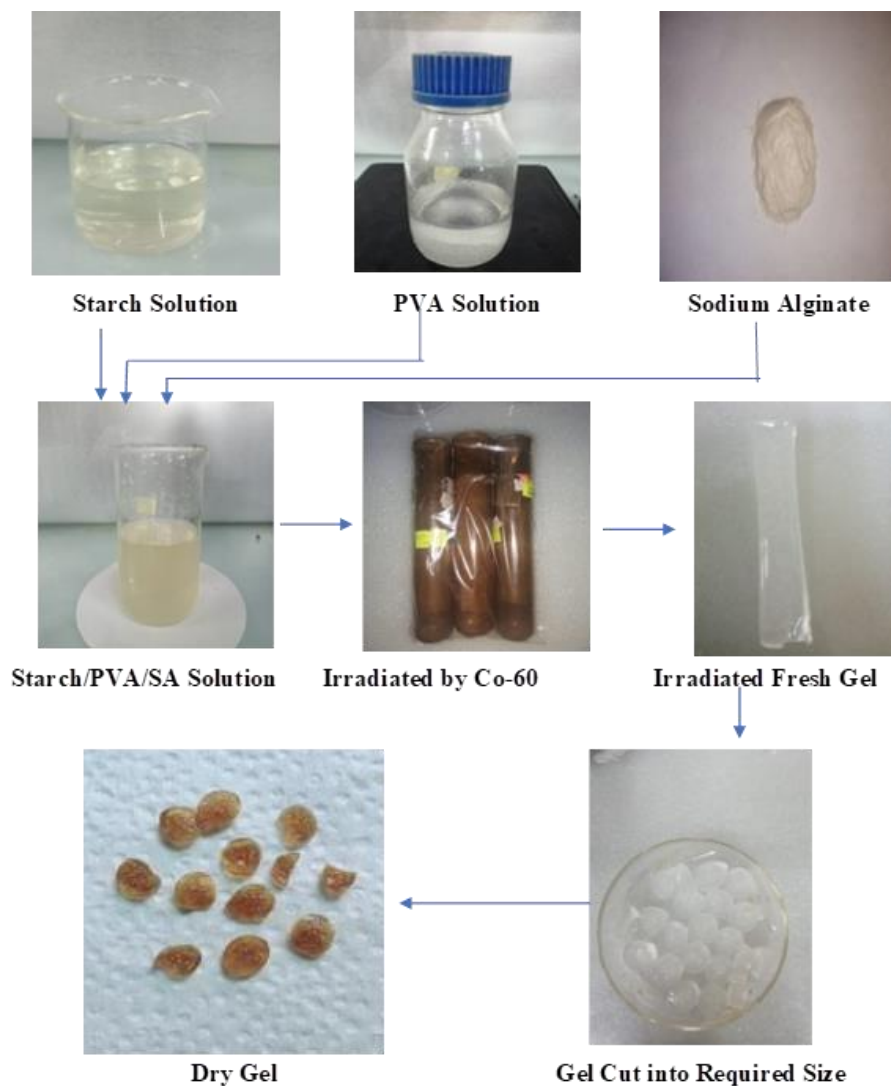


**Figure 1** Preparation of hydrogel by gamma radiation.

## 2.3 Characterization

### 2.3.1 FTIR Analysis

FTIR spectra of PVA/Starch/SA hydrogels were recorded with a Fourier Transform Infrared Spectrometer (model: Shimadzu FT-IR-8400S, Japan). The dried samples were grounded with KBr and then pressed under high pressure to form transparent disks, and disks were placed in the sample holder for recording the spectrum. The wave number range was 4000-800  $\text{cm}^{-1}$ .

### 2.3.2 Measurement of Gel Fraction

To extract the soluble fraction, the constant weight of the dried gel sample was placed in a beaker with water and left at room temperature for 24 hours. In an oven set at 45°C, the gel samples were dried to a consistent weight. The gel fractions of samples were estimated as follows.

$$\text{Gel fraction (\%)} = (W_0 - W_1) \times 100 \quad (1)$$

$W_1$  is the weight of dried gel after extraction, and  $W_0$  is the initial weight of dried gel.

### 2.3.3 Swelling Measurement

The gel samples were submerged in distilled water at room temperature after drying to a consistent weight. The samples were weighed periodically after using a filter paper to remove extra water from the hydrogel's surface. The following equation is used to calculate the swelling ratio of samples:

$$\text{Swelling Ratio (\%)} = \left[ \frac{(W_t - W_1)}{W_1} \right] \times 100 \quad (2)$$

$W_t$  is the weight of the swollen gel sample at the time  $t$ , and  $W_1$  is the initial weight of the dried gel.

### 2.3.4 pH-Dependent Swelling

For buffer solutions ranging from pH 3 to 5, 0.1 M acetic acid and 0.1 M sodium acetate were employed, and for buffer solutions ranging from pH 7 to 9, 0.1 M  $\text{Na}_2\text{HPO}_4$  and 0.1 M HCl were used. Hydrogel samples (PVA/Alginate/Starch blend) swelled for 24 hours in buffer solutions of various pH levels at room temperature. The following equation was used to calculate the swelling ratio (S):

$$S = \frac{W_t - W_i}{W_i} \times 100 \quad (3)$$

$W_t$  is the weight of swollen gel after hydration for 24 hr, and  $W_i$  is the initial weight of the dry gel.

### 2.3.5 Measurement of Cross-Linked Density

Network parameters as the cross-linked polymers are the average molecular weight between two consecutive crosslink ' $M_c$ ', directly related to the crosslink density. The molar mass  $M_c$ , was calculated by using the Flory-Rehner equation, given as

$$M_c = - \frac{d_p v_{2,s} (V_{2,s}^{\frac{1}{3}} - \frac{V_{2,s}}{2})}{\ln(1 - V_{2,s}) + V_{2,s} + \chi V_{2,s}^2} \quad (4)$$

It is also reasonable to define that the volume fraction of the polymer  $V_{2,s}$  (ml/mol) indicates the capacity of hydrogel to allow the diffusion of the solvent into the network structure followed by the equation:

$$V_{2,s} = \left[ 1 + \frac{d_p}{d_s} \left( \frac{M_a}{M_b} - 1 \right) \right]^{-1} \quad (5)$$

$d_p$  and  $d_s$  are the densities (gm/ml) of the polymer and solvent, respectively.  $M_a$  and  $M_b$  are the masses of swollen and dry gels, respectively. Here,  $\chi$  is the Flory- Huggins polymer interaction parameter. The following equation also calculated  $\chi$  :

$$\chi = \frac{\ln(1 - V_{2,s}) + V_{2,s}}{V_{2,s}^2} \quad (6)$$

The following equation is used to determine the cross-linked density where  $q$  is defined as the mole fraction of cross-linked units, and  $\rho$  is the density of the polymer.

$$q = \frac{\rho}{M_c} \quad (7)$$

### 2.3.6 Determination of Dye Adsorption

The optical density of absorption of the colored test solutions is frequently measured using the visible spectrophotometer. The Beer-Lambert law is the foundation for the visual spectrophotometric concentration determination method. In this investigation, the concentration of the dye solution was assessed using a UV-visible spectrophotometer. Methylene blue dye was dissolved in distilled water. Dye solutions were applied to the hydrogels. Periodically, residual dye concentration in aqueous solution was assessed by UV-visible spectroscopy (UV- 1800 Series, Shimadzu, Japan). The following equation gives the equilibrium adsorption capacity,  $q_e$  (mg/g).

$$q_e = \frac{(C_0 - C_e)}{W} v \quad (8)$$

Where  $C_0$  and  $C_e$  are the concentration of dye in the initial solution and after adsorption of a certain period, respectively (mg/L),  $V$  is the volume of solution (L), and  $W$  is the weight of the hydrogel (g) [27].

## 3. Result and Discussion

### 3.1 Optimization of Poly Vinyl Alcohol/Sodium Alginate/Starch Hydrogel Composition at 30 kGy

By keeping the PVA content constant at 5% and the sodium alginate content at 1%, the starch content of the PVA/Starch/SA hydrogel was optimized (Table 1). A radiation dose (30 kGy) was used to create these hydrogels. The hydrogels' gel fraction and swelling ratio were then evaluated to optimize starch content.

**Table 1** Feed composition at radiation dose 30 kGy for the prepared hydrogel.

Sample	PVA (%)	Sodium Alginate (%)	Starch (%)
PAS-0	5	1	0
PAS-0.25	5	1	0.25
PAS-0.5	5	1	0.5
PAS-1	5	1	1

#### 3.1.1 Effect of Starch on Swelling Ratio

The hydrophilicity of the polymer chains affects the swelling ratio of the hydrogel. The effect of starch content is depicted in Figure 2. The swelling ratio rose with starch concentration up to 0.25%.

The swelling ratio values climbed from 2394 to 3673.14 percent before dropping to 3140 percent at 30 kGy. When 0.25% of starch was added it increased the hydrophilicity of the hydrogel. Therefore, swelling increased. However, adding more starch caused cross-linking in the hydrogel, and there swelling was reduced. Water absorption is a crucial characteristic of the manufacture of high-quality adsorbent hydrogels. Figure 3 shows the hydrogel image before and after swelling.

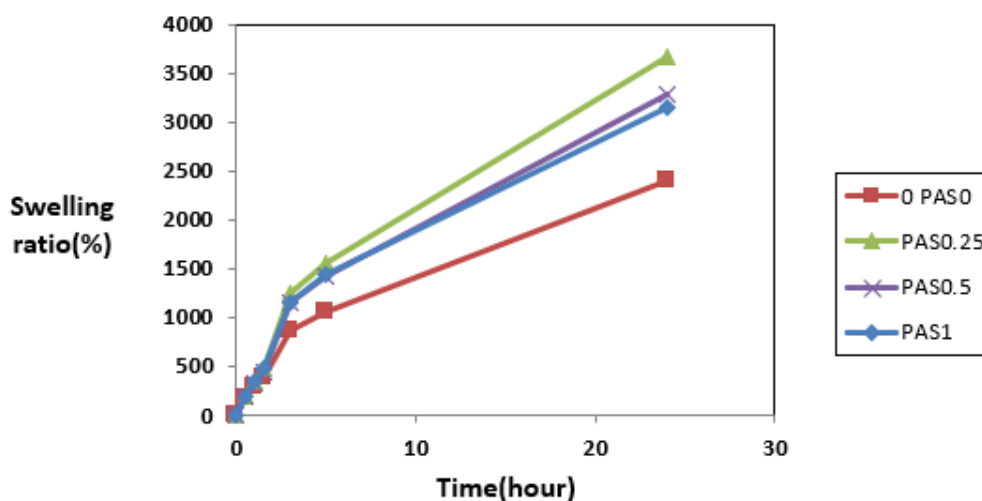


**Figure 2** Effect of starch concentration on swelling ratio of PVA/Starch/SA hydrogels at 30 kGy.

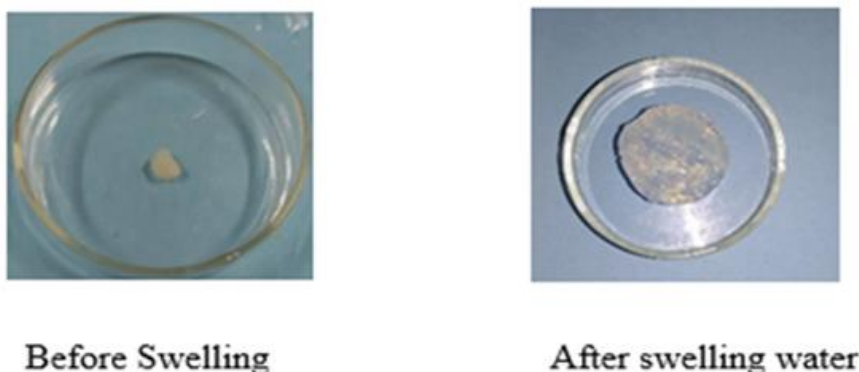


**Figure 3** Hydrogels before and after swelling.

### 3.1.2 Effect of Starch Concentration on Gel Fraction

Figure 4 shows that after adding starch (0.25%), the gel fraction initially reduces modestly but then increases as starch concentration increases—a rise in gel fraction from 87.21% to 89.03%. Highly cross-linked hydrogels have smaller surface pores, preventing water from penetrating deeper into the gel matrix. 0.25% starch content was identified as the optimal starch concentration for our subsequent investigation, considering the swelling ratio and gel fraction. MB adsorption is expected to increase when the swelling ratio rises. Therefore, 0.25% starch content having a reasonable gel fraction (87.21%) with a high swelling ratio is selected for further study.

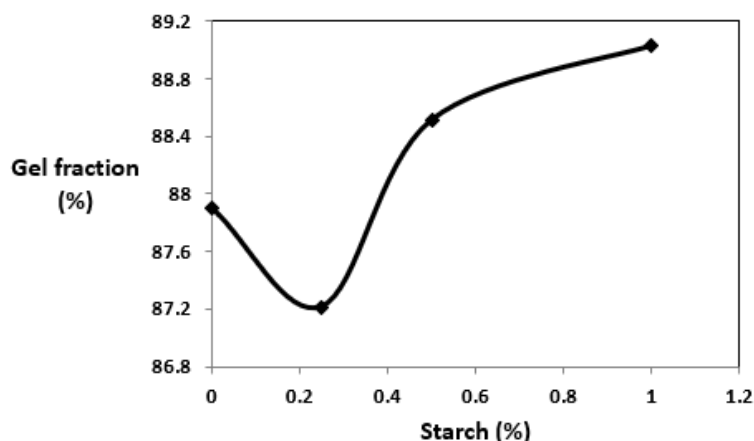


**Figure 4** Effect of starch content on gel fraction of PVA/Starch/SA hydrogels at 30 kGy.

### 3.2 Effect of Radiation Dose on Swelling Ratio of Optimized Hydrogel

PVA/Starch/SA-0.25 hydrogel was made using radiation doses of 20 kGy, 25 kGy, 30 kGy, 35 kGy, and 40 kGy. Figure 5 shows that the swelling ratio drops from 4326.17 to 3298.63 percent when the irradiation dose increases from 20 to 40 kGy. When in contact with water, hydrogel expands rather than breaking down. It is capable of holding water inside its network. Due to the breakdown of starch molecules at high radiation doses, an increase in radiation doses causes a drop in the swelling ratio.

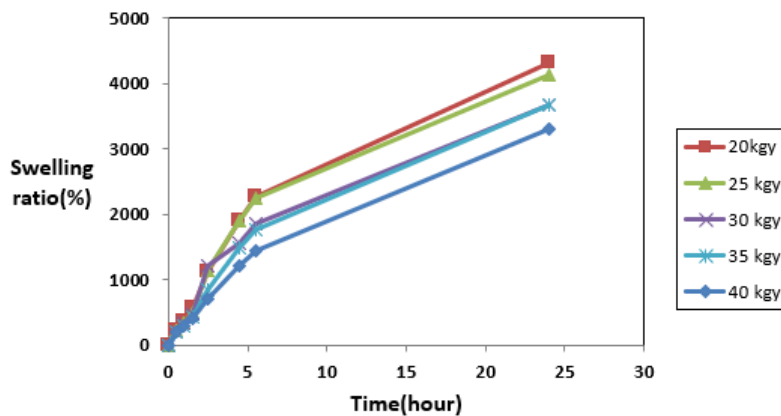


**Figure 5** Effect of radiation doses on a swelling ratio of PVA/Starch/SA-0.25 hydrogel.

### 3.3 Effect of Radiation Dose on Gel Fraction of Optimized Hydrogel

Figure 6 demonstrates how the gel fractions of the hydrogel rose with increasing radiation doses, reaching a maximum of 90.71% at 40 kGy. The image makes it evident that there is a trend for the gel fraction to grow from 20 to 40 kGy. The concentration of free radicals within a monomer/polymer system increases as the radiation dosage passes through it. It is well known that the free radical causes cross-linking. Therefore, the cross-linking between polymer chains increases the gel fraction when the radiation dose rises. At 30 kGy, PAS 0.25 hydrogel was chosen for further study because the 20 kGy and 25 kGy PAS hydrogels were quite thick and had low gel strengths.



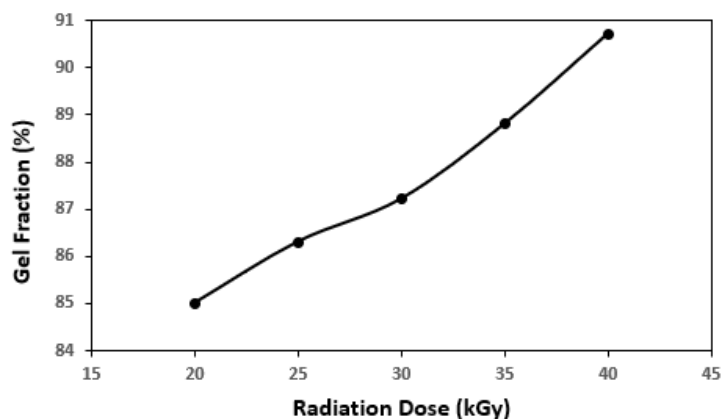


**Figure 6** Effect of radiation doses on gel fraction of PAS 0.25 hydrogels.

### 3.4 Effect of pH on Swelling Ratio

The findings of the study of the % swelling with various pH values 3, 5, 7, and 9 are displayed in Figure 7. It demonstrates that as the pH of the medium increased, the proportion of equilibrium water swelling dramatically increased. When the pH was changed from pH 3 to pH 5, the percentage of equilibrium swelling for PVA/Starch/SA-0.25 hydrogel significantly increased from 1962% to 4070%. After pH 5 the swelling ratio remained almost constant. The complex formation took place at low pH, and nearly little osmotic swelling pressure was noticed in the standard pH solution. Carboxylate (COO<sup>-</sup>) and (-OH) cause a decrease in hydrogen bonding along the network chains at higher pH levels. High swelling ratios and a more hydrophilic polymer network were produced. This also promotes faster polymer chain mobility, improving swelling rate and swelling ratio. It is expected that dye adsorption will also be higher at high pH.

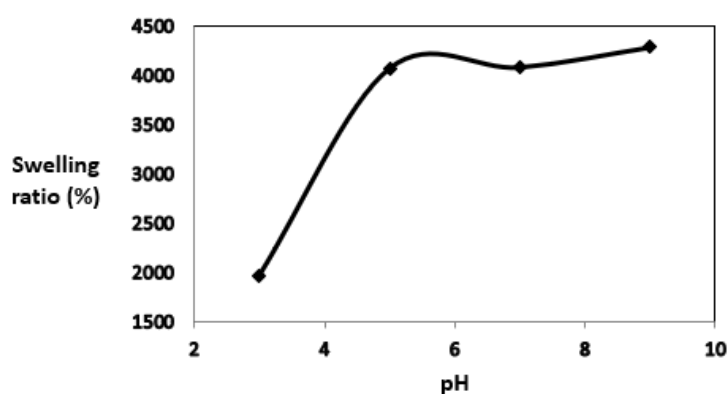


**Figure 7** Effect of pH on a swelling ratio of PAS-0.25 hydrogels.

### 3.5 Cross-linking Density of PAS-0.25 Hydrogels

The swelling ratio reveals how much a polymer has been cross-linked. The swelling ratio dropped as the cross-linked density of a polymer increased because there was less open area for free solvent to enter. The cross-linking density of hydrogels made from PAS-0.25 at radiation doses of 20 kGy to 40 kGy is shown in Figure 8. Polymer networks are more compact when they have a lower swelling capacity. In other words, hydrogels exhibiting significant swelling have more potential to absorb

water because of lower cross-linking densities. The cross-linking density, therefore, increased with radiation exposure.

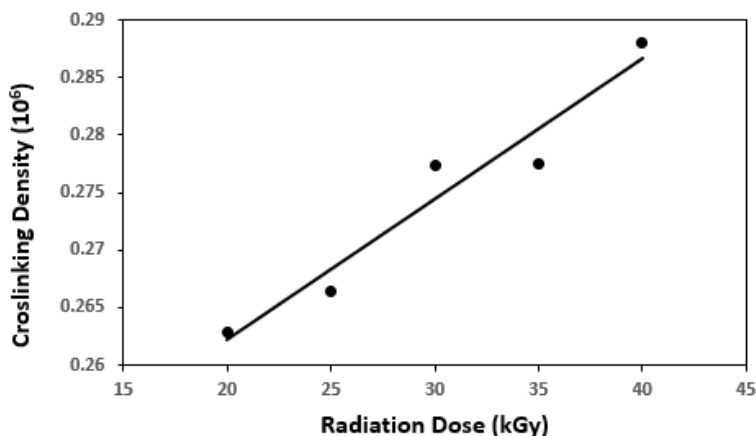


**Figure 8** Effect of radiation doses on crosslinking density of PAS-0.25 hydrogel.

### 3.6 FTIR Analysis

Figure 9 shows the IR spectra of PAS hydrogel. The bands of pristine alginate were associated with the stretching OH vibrations at  $3234\text{ cm}^{-1}$  and  $1263\text{ cm}^{-1}$ , asymmetric and symmetrical vibration of the carbonyl group ( $\text{COO}^-$ ) at  $1606\text{ cm}^{-1}$  and  $1413\text{ cm}^{-1}$ , respectively. A peak at  $3234\text{ cm}^{-1}$  and  $1413\text{ cm}^{-1}$  represents the characteristic OH from PVA alcohol, and a rise at  $2881\text{ cm}^{-1}$  represents the stretching band of  $\text{CH}_2$  and  $\text{CH}_3$  signals. The bands of C–C–C ( $1085\text{ cm}^{-1}$ ) and C–O–C ( $1028\text{ cm}^{-1}$ ) correspond to the alginate glycosidic bond. The peak at  $3383\text{ cm}^{-1}$  was attributed to the stretching vibration of starch hydroxyl.

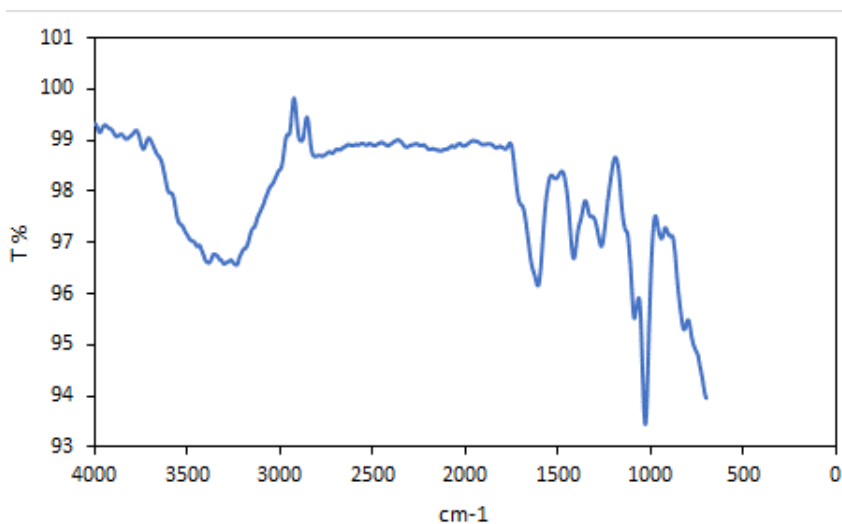


**Figure 9** FTIR spectrum of PVA/Starch/SA.

### 3.7 Adsorption Study

The hydrogel was prepared using a radiation cross-linking technique. The prepared hydrogel was used for MB adsorption. Picture of \hydrogel after dye adsorption is shown in Figure 10.

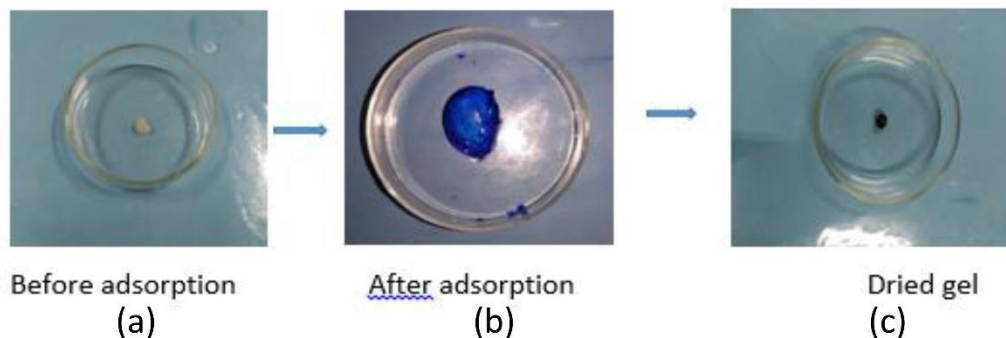


**Figure 10** MB dye adsorption (a) Before adsorption (b) After adsorption (c) Dried gel.

### 3.7.1 Effect of Adsorbent Dosage

Various adsorbent dosages (0.01-0.06 g) were used to determine how an adsorbent dose affected the adsorption of MB (with a concentration of 25 ppm). The plots of adsorption capacity (mg/g) vs various adsorbent dosages are displayed in Figure 11. Figure 11 shows that as the adsorbent dosage increases, the amount of adsorbent material per unit of adsorbent decreases. This may be because more active sites are on the adsorbent's surface. This result suggests to take a small amount of adsorbent dose as much as possible. However, to facilitate handling, the adsorbent dose of 0.02 g of adsorbent was chosen for additional adsorption studies.

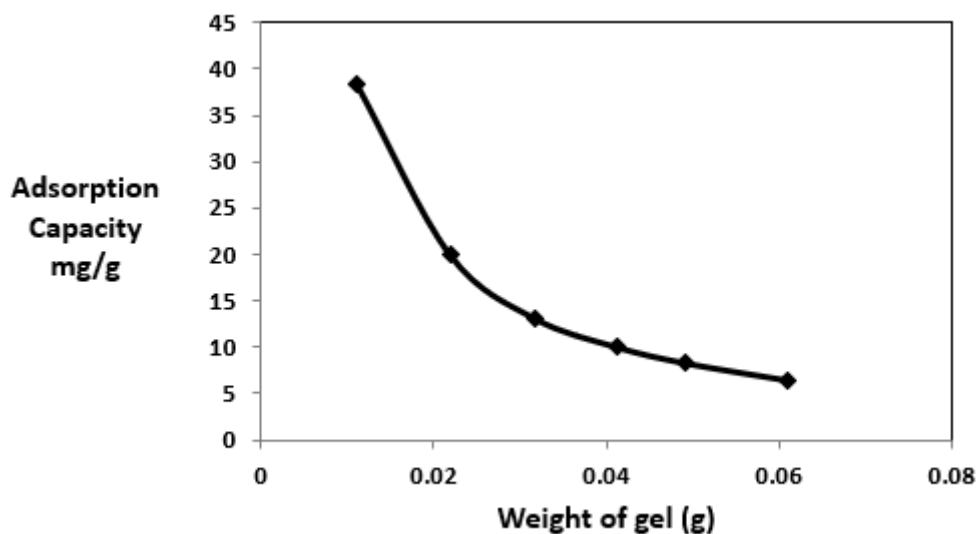


**Figure 11** Effect of PAS adsorbent doses on adsorption capacity (mg/g).

### 3.7.2 Adsorption Kinetics and Mechanism

On the elimination of MB, the influence of contact time was investigated. It was shown that as contact time increased, the capacity for equilibrium adsorption and the elimination of MB both increased. Within 6 hours of contact time, equilibrium was reached. Because of its porous surface and significant water absorption capabilities, hydrogel is undoubtedly one of the finest options for dye removal. In this experiment, 0.0801 g of hydrogel was dipped in 100 ml of a 100 ppm methylene

blue (MB) dye solution. The dye concentration during adsorption was recorded after particular time intervals and was assessed by UV spectroscopy.

To check the fitting of kinetic data, the pseudo-first-order [28] and pseudo-second-order kinetic equations [29] were used, as shown in Figure 12 and Figure 13, respectively. The linear form of a pseudo-first-order kinetic equation is given as follows:

$$\ln(q_e - q_t) = \ln q_e - K_1 t \tag{9}$$

And the linear form of the pseudo-second order kinetic equation is given as follows:

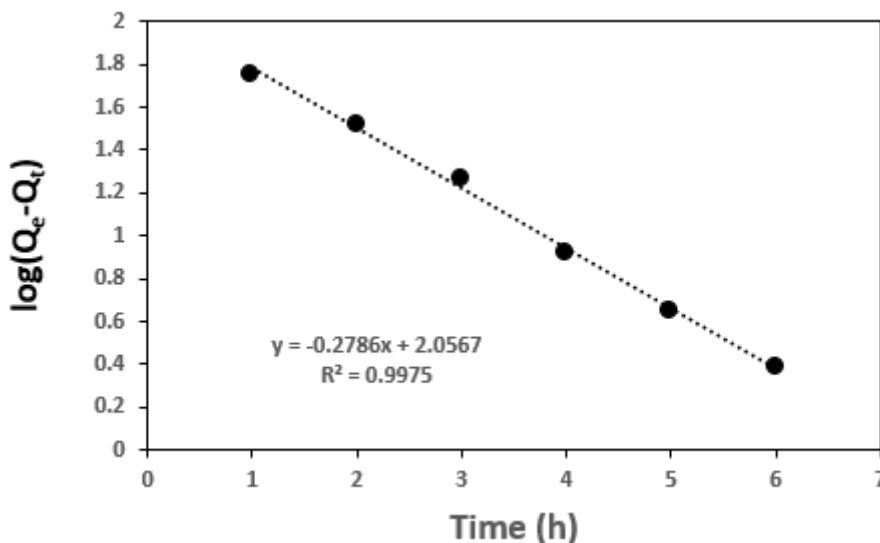


Figure 12 Pseudo 1<sup>st</sup> order kinetics of MB adsorption.

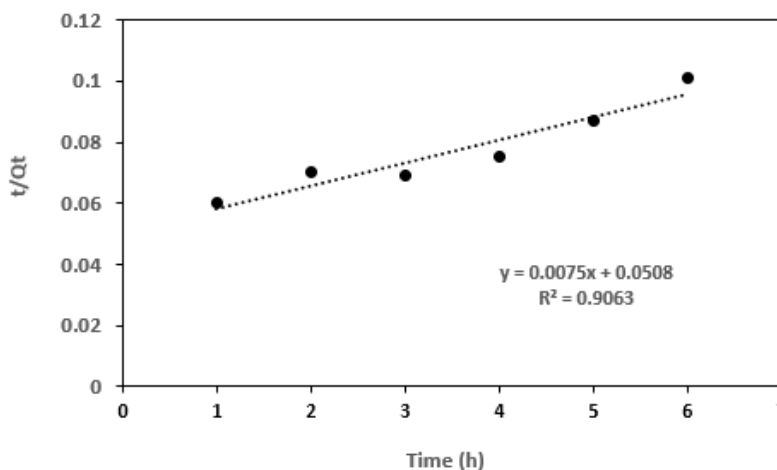


Figure 13 Pseudo 2<sup>nd</sup> order kinetics of MB adsorption.

$$\frac{t}{q_e} = \frac{1}{k_2 q_e^2} + \frac{1}{q_e} \cdot t \tag{10}$$

Where  $q_e$  is the equilibrium adsorption capacity (mg/g),  $q_t$  is the adsorption capacity at time  $t$  (mg/g),  $k_1$  is the pseudo first-order rate constant ( $\text{min}^{-1}$ ),  $t$  is the time (min),  $k_2$  is the pseudo-second-order rate constant (g/mg min), and  $b = k_2 \cdot q_e^2$ , is the initial adsorption rate ( $\text{mg g}^{-1} \text{min}^{-1}$ ).

R<sup>2</sup> value of pseudo 1<sup>st</sup> order is 0.99 which is higher than R<sup>2</sup> value of pseudo 2<sup>nd</sup> order 0.90. So, the pseudo 1st-order kinetic model fits with the experimental kinetic data.

### 3.7.3 Adsorption Isotherm of MB Dye

An adsorption isotherm is the relationship between the amount of adsorbate adsorbed on the adsorbent and the concentration of dissolved adsorbate in the liquid at equilibrium. The Freundlich and Langmuir isotherms are the most popular methods for describing an adsorbent's adsorption characteristics. The isotherm studies used 0.02 gm of hydrogel in 25 ml dye solutions with concentrations ranging from 50, 100, 200, 300, 400, and 500 ppm.

Langmuir Isotherm. Langmuir model [30] is widely used to apply the adsorption isotherm based on the monolayer adsorption on the surface of the adsorbent. The linear form of the Langmuir equation is provided as:

$$\frac{1}{q_e} = \frac{1}{q_m C_e K_L} + \frac{1}{q_m} \quad (11)$$

The essential feature of the Langmuir isotherm can be expressed in terms of a dimensionless constant called separation factor ( $R_L$ , also called equilibrium parameter), which is defined by the following equation:

$$R_L = \frac{1}{1 + K_L C_0} \quad (12)$$

where  $C_0$  (mg/L) is the initial adsorbate concentration. The value of  $R_L$  which indicates the shape of the isotherms to be either unfavorable ( $R_L > 1$ ), linear ( $R_L = 1$ ), favorable ( $0 < R_L < 1$ ) or irreversible ( $R_L = 0$ ) [31].  $K_L$  was 0.1322. The separation factor ( $R_L$ ) was found 0.0364. The obtained  $R_L$  values were in the range of 0-1, indicating favorable MB adsorption onto the PAS-based hydrogel [32].

The Langmuir isotherm plot for MB adsorption is shown in Figure 14.

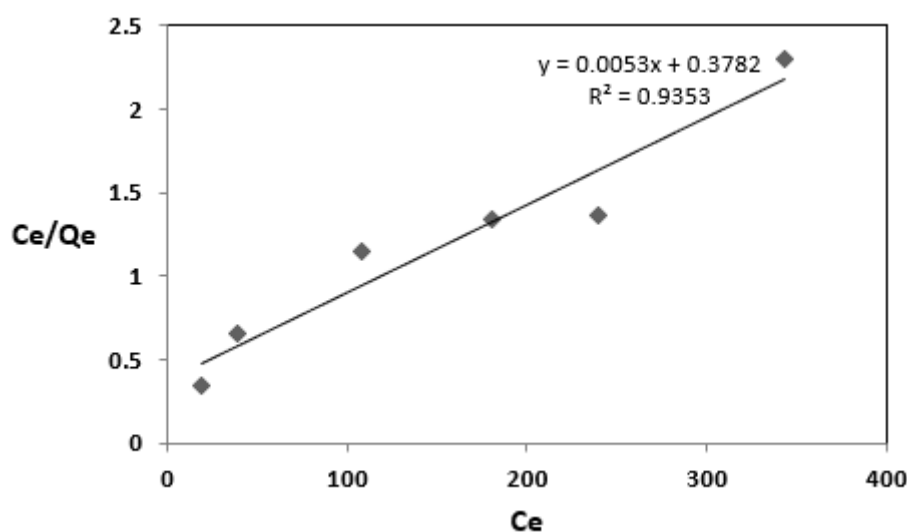


**Figure 14** Langmuir isotherm of MB adsorption.

**Freundlich Isotherm.** The most critical multisite adsorption isotherm for heterogeneous surfaces is the Freundlich adsorption isotherm, and the linear form of this isotherm is expressed as [33]:

$$\ln q_e = \ln K_f + \frac{1}{n} \ln C_e \quad (13)$$

$q_e$  is solid phase equilibrium concentration (mg/g),  $C_e$  is liquid phase equilibrium concentration (mg/L), and  $K_f$  and  $n$  are Freundlich constants. The value of 'n' indicates the feasibility of the adsorption process. Freundlich isotherm plot for MB adsorption is shown in Figure 15.

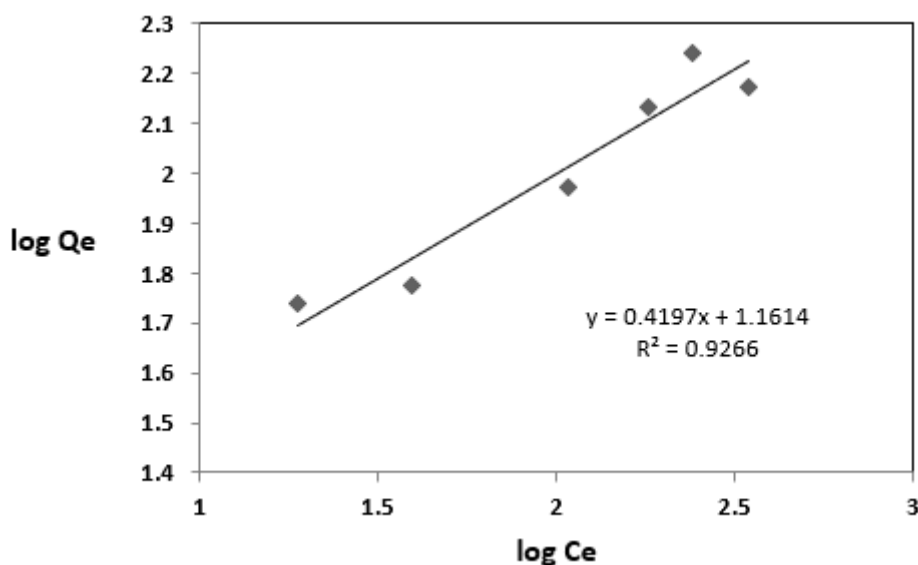


**Figure 15** Freundlich isotherm of MB adsorption.

$K_f=14.59$  and  $n = 2.3866$ . It is said that if the value of  $n$  is in the range of 2-10 favorable adsorption is shown, 1-2 represents moderately difficult, and less than 1 indicates poor adsorption characteristics. It can be seen that the coefficient of adsorption ( $R^2$ ) is lower in the Freundlich isotherm. Langmuir isotherm shows a higher  $R^2$  value. Therefore, it can be presumed that the adsorption of MB on PAS-based hydrogel follows Langmuir adsorption model, which indicates the best linearized isotherm model. This indicates that a monolayer adsorption process has been carried out on the homogeneously distributed active sites of the hydrogels.

### 3.7.4 Thermodynamics Studies

The thermodynamic parameters such as free energy change ( $\Delta G^0$ ), enthalpy change ( $\Delta H^0$ ), and entropy change ( $\Delta S^0$ ) were obtained from the van't Hoff equation [34, 35]:

$$\Delta G^0 = -2.303RT \log k_d \quad (14)$$

$$k_d = \frac{q_e}{c_e} = \frac{\Delta S^0}{2.303R} - \frac{\Delta H^0}{2.303RT} \quad (15)$$

Where  $\Delta H^0$  in kJ/mol/K represents the standard enthalpy change;  $\Delta G^0$  in kilojoules per mole is the variation of standard Gibb's free energy;  $\Delta S^0$  is the standard entropy variation in kilojoules per

mole;  $k_d$  is the Langmuir constant at a given temperature;  $R$  in J/mol/K is the molar gas constant; and  $K$  is the Kelvin temperature. The plot  $\log k_d$  against  $1/T$  (Figure 10b) could be applied to calculate the values of  $\Delta H^\circ$ ,  $\Delta S^\circ$ , and  $\Delta G^\circ$  at different temperatures.

For the temperature study, 0.0201 g PAS gel was placed in 25 ml 100 ppm MB dye solution and observed after 5 hours. The effect of increasing temperature on the adsorption study was performed in the range of 276 K, 295 K, and 333 K under constant parameters at equilibrium conditions. The result is shown in Figure 16.

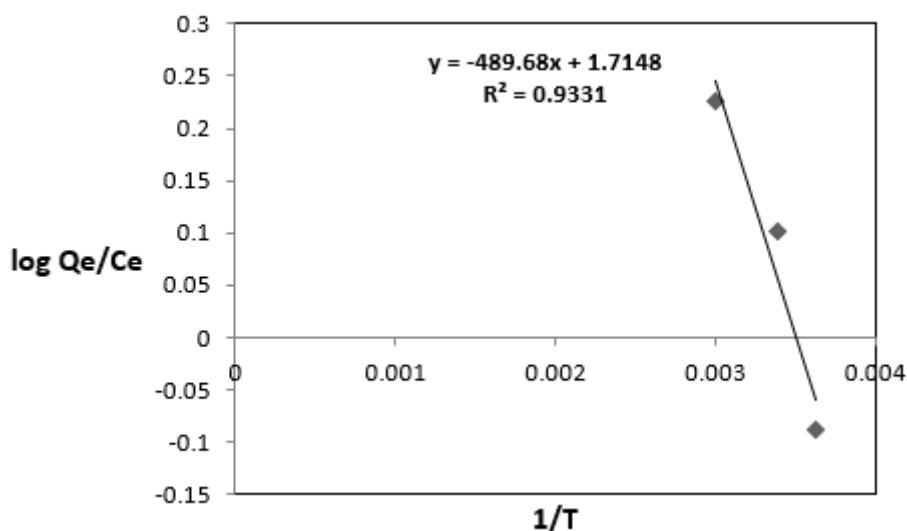


**Figure 16** Thermodynamics study of MB adsorption.

The positive value of  $\Delta H^\circ$  (4.070534 KJ mol<sup>-1</sup>) indicated that the adsorption of MB dye molecules onto PAS gel was endothermic. The value of  $\Delta S^\circ$  was found to be positive 14.250 J K<sup>-1</sup> mol<sup>-1</sup>, indicating the increase in disorder at the solid-liquid interface during the adsorption process. The calculated  $\Delta G^\circ$  values showed a decrease with increasing the temperature from 276 K to 333 K, indicating that the adsorption of MB dye molecules onto PAS gel is more feasible and spontaneous at high temperatures. Thermodynamic parameters are shown in Table 2.

**Table 2** Thermodynamics parameters.

Dye	$\Delta H^\circ$ (KJ mol <sup>-1</sup> )	$\Delta S^\circ$ (J K <sup>-1</sup> mol <sup>-1</sup> )	$\Delta G^\circ$ (KJ mol <sup>-1</sup> )		
			276 K	295 K	333 K
MB	4.070	14.250	-3.929	-4.200	-4.741

### 3.7.5 pH Study on MB Adsorption

For 24 hours, 0.0212 g of PAS-0.25 gels were dissolved in 25 ml of a 100 ppm MB dye solution. Results are shown in Figure 17. The amount of fixed ionized -OH groups increases as the pH of the solution (3 to 9) rises because the adsorbent surface becomes more negatively charged due to being deprotonated. Two different electrostatic forces are produced as a result of this: (1) electrostatic repulsion between adjacent ionized groups of polymer networks, which causes the polymer chains in the hydrogel structure to expand, and (2) electrostatic interaction between the positively charged dye and negatively charged hydrogel network. The MB dye molecules and the hydrogel networks

form an ionic combination, enhancing the dye adsorption (mg/g). Comparison of methylene blue absorption capacity of the prepared adsorbent with other adsorbents is shown in Table 3.

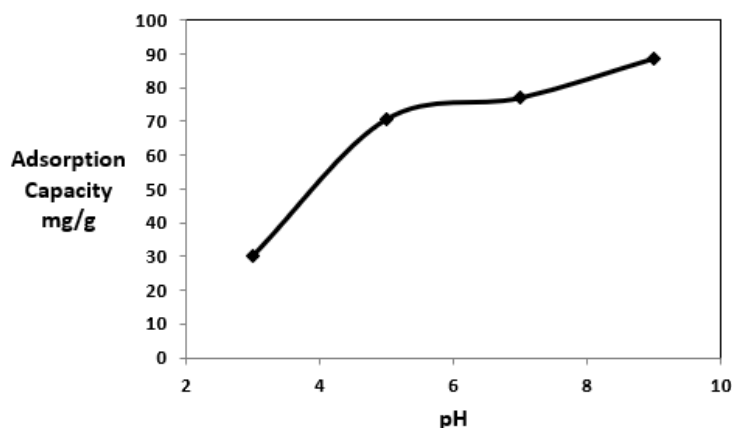


**Figure 17** Effect of pH of MB adsorption.

**Table 3** Methylene blue absorption capacity of the prepared adsorbent compared with other adsorbents.

Absorbent	Absorption capacity (mg/g)
PAS hydrogel [present study]	174.83
Carbon monolith [36]	127
Nanocrystalline cellulose [36]	101
Wheat shells [37]	21.50
Gulmohar (Delonix regia) plant leaf [38]	186.22
Tea waste [39]	85.16
Thermally activated coir pith carbon [40]	5.87

### 3.8 Desorption Study

After the adsorption of MB dye on the PAS hydrogel, the adsorbents were subjected to desorption using 2 M HCl solution for 24 hours. The desorption ratio was satisfactory, about 90%.

## 4. Conclusion

In the current study, Co-60 gamma radiation was used to create a novel cross-linked hydrogel (PVA/Sodium Alginate/Starch). The effects of factors like irradiation dose and composition ratio on the characteristics of the manufactured hydrogels, including gel content and swelling behavior, were carefully examined. 30 kGy radiation dose and 0.25% were selected as the optimal dose and starch content, respectively. By using FTIR, the produced hydrogel was identified. This hydrogel's ability to remove the colour methylene blue was investigated while taking isotherm and kinetic factors into account. The pseudo-first-order kinetic model and the MB dye adsorption experimental data onto the PAS hydrogels were in good agreement. The adsorption process was endothermic and spontaneous. The ideal contact duration and pH for MB adsorption were 24 hours and 9,



respectively. The maximum adsorption capacity determined from Langmuir model was 174.83 mg g<sup>-1</sup>. The treatment of waste-water containing MB dye may benefit from our work.

## **Acknowledgments**

The authors would like to express their appreciation to the International Atomic Energy Agency (IAEA) for their assistance with the technical aspects of this study. The contributions of the Institute of Food and Radiation Biology at Bangladesh's Atomic Energy Research Establishment are also worthy of mention.

## **Author Contributions**

Depok Chandra Shil, Nazia Rahman and Shahnaz Sultana did the experimental work. Md. Nabul Sardar, Puja Majumder, Fataha Nur Robel helped in experiment design. Depok Chandra Shil and Nazia Rahman wrote the manuscript.

## **Competing Interests**

About this article, the authors state that they have no competing interests to disclose.

## **References**

1. Mirzaie M, Rashidi A, Tayebi HA, Yazdanshenas ME. Optimized removal of acid blue 62 from textile waste water by SBA-15/PAMAM dendrimer hybrid using response surface methodology. *J Polym Environ*. 2018; 26: 1831-1843.
2. Pekakis PA, Xekoukoulotakis NP, Mantzavinos D. Treatment of textile dyehouse wastewater by TiO<sub>2</sub> photocatalysis. *Water Res*. 2006; 40: 1276-1286.
3. Rauf MA, Ashraf SS. Fundamental principles and application of heterogeneous photocatalytic degradation of dyes in solution. *Chem Eng J*. 2009; 151: 10-18.
4. Cao J, Tan Y, Che Y, Xin H. Novel complex gel beads composed of hydrolyzed polyacrylamide and chitosan: An effective adsorbent for the removal of heavy metal from aqueous solution. *Bioresour Technol*. 2010; 101: 2558-2561.
5. Huang L, Xiao C, Chen B. A novel starch-based adsorbent for removing toxic Hg(II) and Pb(II) ions from aqueous solution. *J Hazard Mater*. 2011; 192: 832-836.
6. Masoumi A, Ghaemy M. Removal of metal ions from water using nanohydrogel tragacanth gum-g-polyamidoxime: Isotherm and kinetic study. *Carbohydr Polym*. 2014; 108: 206-215.
7. Lanthong P, Nuisin R, Kiatkamjornwong S. Graft copolymerization, characterization, and degradation of cassava starch-g-acrylamide/itaconic acid superabsorbents. *Carbohydr Polym*. 2006; 66: 229-245.
8. Crini G. Non-conventional low-cost adsorbents for dye removal: A review. *Bioresour Technol*. 2006; 97: 1061-1085.
9. Xie G, Shang X, Liu R, Hu J, Liao S. Synthesis and characterization of a novel amino modified starch and its adsorption properties for Cd(II) ions from aqueous solution. *Carbohydr Polym*. 2011; 84: 430-438.
10. Kumar M, Tripathi BP, Shahi VK. Crosslinked chitosan/polyvinyl alcohol blend beads for removal and recovery of Cd(II) from wastewater. *J Hazard Mater*. 2009; 172: 1041-1048.

11. Zhu HY, Fu YQ, Jiang R, Yao J, Xiao L, Zeng GM. Novel magnetic chitosan/poly (vinyl alcohol) hydrogel beads: Preparation, characterization and application for adsorption of dye from aqueous solution. *Bioresour Technol.* 2012; 105: 24-30.
12. Zhou Y, Fu S, Zhang L, Zhan H, Levit MV. Use of carboxylated cellulose nanofibrils-filled magnetic chitosan hydrogel beads as adsorbents for Pb(II). *Carbohydr Polym.* 2014; 101: 75-82.
13. Sin LT, Bee ST, Tee TT, Kadhum AA, Ma C, Rahmat AR, et al. Characterization of  $\alpha$ -tocopherol as interacting agent in polyvinyl alcohol–Starch blends. *Carbohydr Polym.* 2013; 98: 1281-1287.
14. Pawar SN. Chemical modification of alginate. In: *Seaweed polysaccharides*. Amsterdam, Netherlands: Elsevier; 2017. pp. 111-155.
15. Zhang MK, Zhang XH, Han GZ. Magnetic alginate/PVA hydrogel microspheres with selective adsorption performance for aromatic compounds. *Sep Purif Technol.* 2021; 278: 119547.
16. Peng XW, Zhong LX, Ren JL, Sun RC. Highly effective adsorption of heavy metal ions from aqueous solutions by macroporous xylan-rich hemicelluloses-based hydrogel. *J Agric Food Chem.* 2012; 60: 3909-3916.
17. Cipriano BH, Banik SJ, Sharma R, Rumore D, Hwang W, Briber RM, et al. Superabsorbent hydrogels that are robust and highly stretchable. *Macromolecules.* 2014; 47: 4445-4452.
18. Ahmed EM. Hydrogel: Preparation, characterization, and applications: A review. *J Adv Res.* 2015; 6: 105-121.
19. Ding R, Yu X, Wang P, Zhang J, Zhou Y, Cao X, et al. Hybrid photosensitizer based on amphiphilic block copolymer stabilized silver nanoparticles for highly efficient photodynamic inactivation of bacteria. *RSC Adv.* 2016; 6: 20392-20398.
20. Lee KY, Mooney DJ. Hydrogels for tissue engineering. *Chem Rev.* 2001; 101: 1869-1880.
21. Zhai D, Liu B, Shi Y, Pan L, Wang Y, Li W, et al. Highly sensitive glucose sensor based on Pt nanoparticle/polyaniline hydrogel heterostructures. *ACS Nano.* 2013; 7: 3540-3546.
22. Li L, Wang Y, Pan L, Shi Y, Cheng W, Shi Y, et al. A nanostructured conductive hydrogels-based biosensor platform for human metabolite detection. *Nano Lett.* 2015; 15: 1146-1151.
23. Malatji N, Makhado E, Modibane KD, Ramohlola KE, Maponya TC, Monama GR, et al. Removal of methylene blue from wastewater using hydrogel nanocomposites: A review. *Nanomater Nanotechnol.* 2021; 11: 18479804211039425.
24. Salunkhe B, Schuman TP. Super-adsorbent hydrogels for removal of methylene blue from aqueous solution: Dye adsorption isotherms, kinetics, and thermodynamic properties. *Macromol.* 2021; 1: 256-275.
25. Shah SS, Ramos B, Teixeira AC. Adsorptive removal of methylene blue dye using biodegradable superabsorbent hydrogel polymer composite incorporated with activated charcoal. *Water.* 2022; 14: 3313.
26. Pereira AG, Rodrigues FH, Paulino AT, Martins AF, Fajardo AR. Recent advances on composite hydrogels designed for the remediation of dye-contaminated water and wastewater: A review. *J Clean Prod.* 2021; 284: 124703.
27. Hassan MR, Chowdhury AB, Islam MT.  $\gamma$ -Irradiated Polyvinyl Alcohol (PVA) and acrylic acid blend hydrogels: Swelling and absorption properties. *Chem Technol Ind J.* 2016; 11: 107-117.
28. Wach RA, Kudoh H, Zhai M, Muroya Y, Katsumura Y. Laser flash photolysis of carboxymethylcellulose in an aqueous solution. *J Polym Sci A Polym Chem.* 2005; 43: 505-518.
29. Al-Assaf S, Phillips GO, Deeb DJ, Parsons B, Starnes H, Von Sonntag C. The enhanced stability of the cross-linked hylan structure to hydroxyl (OH) radicals compared with the uncross-linked

- hyaluronan. *Radiat Phys Chem.* 1995; 46: 207-217.
30. Febrianto J, Kosasih AN, Sunarso J, Ju YH, Indraswati N, Ismadji S. Equilibrium and kinetic studies in adsorption of heavy metals using biosorbent: A summary of recent studies. *J Hazard Mater.* 2009; 162: 616-645.
  31. Zhai M, Yoshii F, Kume T, Hashim K. Syntheses of PVA/starch grafted hydrogels by irradiation. *Carbohydr Polym.* 2002; 50: 295-303.
  32. Lugao AB, Malmonge SM. Use of radiation in the production of hydrogels. *Nucl Instrum Methods Phys Res B.* 2001; 185: 37-42.
  33. Ayawei N, Ebelegi AN, Wankasi D. Modelling and interpretation of adsorption isotherms. *J Chem.* 2017; 2017: 3039817.
  34. Li R, Liang W, Li M, Jiang S, Huang H, Zhang Z, et al. Removal of Cd(II) and Cr(VI) ions by highly cross-linked Thiocarbohydrazide-chitosan gel. *Int J Biol Macromol.* 2017; 104: 1072-1081.
  35. Rahman N, Hossen MS, Miah AR, Marjub MM, Dafader NC, Shahnaz S, et al. Removal of Cu(II), Pb(II) and Cr(VI) ions from aqueous solution using amidoximated non-woven polyethylene-g-acrylonitrile fabric. *J Environ Health Scie Eng.* 2019; 17: 183-194.
  36. He X, Male KB, Nesterenko PN, Brabazon D, Paull B, Luong JH. Adsorption and desorption of methylene blue on porous carbon monoliths and nanocrystalline cellulose. *ACS Appl Mater Interfaces.* 2013; 5: 8796-8804.
  37. Bulut Y, Aydin H. A kinetics and thermodynamics study of methylene blue adsorption on wheat shells. *Desalination.* 2006; 194: 259-267.
  38. Ponnusami V, Gunasekar V, Srivastava SN. Kinetics of methylene blue removal from aqueous solution using gulmohar (*Delonix regia*) plant leaf powder: Multivariate regression analysis. *J Hazard Mater.* 2009; 169: 119-127.
  39. Uddin MT, Islam MA, Mahmud S, Rukanuzzaman M. Adsorptive removal of methylene blue by tea waste. *J Hazard Mater.* 2009; 164: 53-60.
  40. Kavitha D, Namasivayam C. Experimental and kinetic studies on methylene blue adsorption by coir pith carbon. *Bioresour Technol.* 2007; 98: 14-21.